The chloride ion penetration mechanism in basalt fiber reinforced concrete under compression after elevated temperatures

applied sciences

MDPI

Article

The Chloride Ion Penetration Mechanism in Basalt Fiber Reinforced Concrete under Compression after Elevated Temperatures

Limin Lu [1,2], Shaohua Wu [3], Yuwen Qin [3], Guanglin Yuan [1,3], Qingli Zhao [4,*] and Jeung-Hwan Doh [5]

1 Jiangsu Key Laboratory of Environmental Impact and Structural Safety in Engineering, China University of Mining & Technology, Xuzhou 221116, China; Limin.lu@cumt.edu.cn (L.L.); YGL65@cumt.edu.cn (G.Y.)
2 Jiangsu Collaborative Innovation Center for Building Energy Saving and Construction Technology, Xuzhou 221116, China
3 School of Mechanics and Civil Engineering, China University of Mining & Technology, Xuzhou 221116, China; ts19030085a31@cumt.edu.cu (S.W.); qinyuwen1@yango.com.cn (Y.Q.)
4 Department of Civil Engineering, Harbin Institute of Technology, Harbin 264209, China
5 School of Engineering and Built Environment, Griffith University, Southport, QLD 4222, Australia; J.Doh@griffith.edu.au
* Correspondence: zhaoqingli@hit.edu.cn

Abstract: Chloride ion penetration frequently leads to steel corrosion and reduces the durability of reinforced concrete. Although previous studies have investigated the chloride ion permeability of some fiber concrete, the chloride ion permeability of the basalt fiber reinforced concrete (BFRC) has not been widely investigated. Considering that BFRC may be subjected to various exposure environments, this paper focused on exploring the chloride ion permeability of BFRC under the coupling effect of elevated temperatures and compression. Results demonstrated that the chloride ion content in concrete increased linearly with temperature. After exposure to different elevated temperatures, the chloride ion content in BFRC varied greatly with increasing stress. The compressive stress ratio threshold for the chloride ion penetration was measured. A calculation model of BFRC chloride ion diffusion coefficient under the coupling effect of elevated temperatures and mechanical damage (loading test) was proposed.

Keywords: basalt fiber reinforced concrete (BFRC); elevated temperature; compression experiment; chloride ion penetration

Citation: Lu, L.; Wu, S.; Qin, Y.; Yuan, G.; Zhao, Q.; Doh, J.-H. The Chloride Ion Penetration Mechanism in Basalt Fiber Reinforced Concrete under Compression after Elevated Temperatures. *Appl. Sci.* **2021**, *11*, 10137. https://doi.org/10.3390/app112110137

Academic Editors: Luis Laim, Aldina Santiago and Nicola Tondini

Received: 23 September 2021
Accepted: 25 October 2021
Published: 29 October 2021

1. Introduction

Elevated temperatures and chloride ion erosion are affecting the durability of concrete structures [1]. Elevated temperatures cause the micro-structure of concrete to deteriorate and decrease impermeability. It is necessary to evaluate the chloride ion penetration resistance of structural concrete after a disaster.

The permeability of chloride ions into concrete is mainly related to the pore structure and cracks [2]. Further, the chloride ion penetration of concrete increases with the increase in the water/cement ratio [3]. Adding fly ash and slag to concrete could improve pore structure and resistance to chloride ion penetration [4]. Djerbi [5] studied the effect of crack width on the chloride ion diffusion coefficient. Wang considered crack tortuosity and orientation and suggested that effective crack width and effective crack density were correlated with the chloride ion diffusivity of cracked concrete [6]. The chloride ion diffusion coefficient, under the action of elevated temperatures, gradually increased with the increase in heating temperature. Additionally, thermal damage reduced the penetration resistance of concrete [7,8].

The load changes the size of concrete pores, and the size of concrete pores, in turn, affects concrete permeability. The chloride ion content decreases as the compressive stress

ratio increases and gradually increases after exceeding the critical stress level [9,10]. Corrosion tests under compressive stress found that concrete's threshold stress ratio at room temperature is about 0.3 [11]. Concrete mixed with glass fiber has a higher resistance to chloride ion permeability than ordinary concrete [12]. Current studies have found that fibers' diameter and volume fraction influences the diffusion of chloride ions in concrete [13]. Incorporating basalt fiber could improve the toughness and impermeability of concrete to a certain extent. Basalt fiber has excellent resistance to alkaline erosion and is suitable for reinforcing the alkaline concrete matrix [14]. Sim et al. [15] and High et al. [16] conducted experimental studies on the high-temperature performance of BFRC and found that the basalt fiber can improve the performance of concrete exposed to elevated temperatures. However, the law of chloride ion penetration under the thermal-load coupling effect of BFRC has yet to be studied.

To clarify the permeability of BFRC under long-term axial load after elevated temperatures, a chloride ion penetration test of BFRC specimen under axial compression was conducted. Fick's second law is widely used to analyze the diffusion law of chloride ions in concrete [17]. A chloride ion diffusion model that considers the influences of different factors was developed by introducing parameters into the formula [18,19]. Based on the results, a calculation model for the chloride ion diffusion coefficient of BFRC under the coupling effect of elevated temperatures and loads was proposed to provide a basis for evaluating the durability and service life of BFRC.

2. Experimental Programs

2.1. Materials

The prismatic specimen with a size of 100 × 100 × 300 mm was selected in this experiment. Additionally, C40 grade concrete mixed with basalt fiber was used. According to the standard (FGJ55-2011) [20], the amount of each component was calculated and determined after trials and adjustments. The mix proportions of the concrete are listed in Table 1.

Table 1. The mix proportions of the concrete.

Type of Concrete	Component Amount (kg/m^3)					Volume Content
	Cement	Water	Sand	Stone	Water Reducer	Basalt Fiber (%)
BFRC	400	175	703.06	1054.59	0.64	0.15

2.2. Experimental Program

The BFRC specimens were first heated to 200 °C, 400 °C, and 600 °C at a heating rate of 10 °C/min, and then cooled in the air to room temperature.

After the heating test, a non-casting surface of the concrete was selected as the chloride ion penetration surface. The remaining five surfaces were sealed with epoxy resin to ensure that the chloride ions was penetratinging in a one-direction. Chlorine salt solution with a concentration of 5% was used to accelerate the natural erosion process. The erosion days of the specimens were 28, 56, and 84 days.

The water-soluble chloride ion content of different depth layers of the concrete specimen was measured after the erosion process. The concrete powder for depth layers from the surface counts: 0–5 mm, 5–10 mm, 10–15 mm, 15–20 mm, 20–25 mm, and 25–30 mm were measured by the DY-2501B chloride ion meter.

2.3. Loading System

To test the mechanism of chloride ion penetration in concrete under continuous axial load, the natural diffusion method was used. Three compressive stress ratios of 0.1, 0.2, and 0.3 times that of the axial compressive strength of the concrete prism were selected. The specimens were soaked in the solution and, at the same time, placed under a constant compressive load supplied by the hoisting jack on top. The hoisting jacks were supported

by a portal frame. In between each hoisting jack and the portal frame, there was a pressure sensor to measure the load and keep it constant during the chloride erosion days. The loading system is shown in Figure 1.

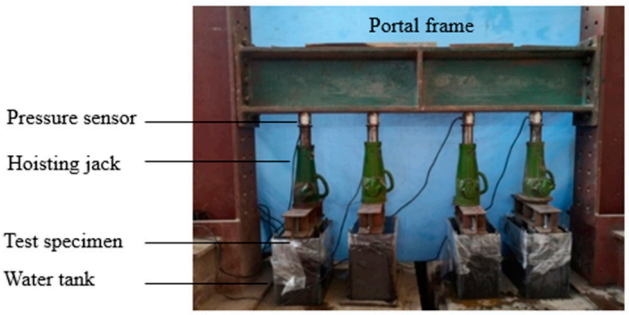

Figure 1. Loading system.

3. Results and Discussion

3.1. Influence of Stress Levels on Chloride Ion Penetration in BFRC

To analyze the influence of stress levels on the chloride ion penetration in BFRC, the chloride ion content of different depth layers of the concrete specimens with respect to different compressive stress ratios were compared. All the selected specimens were soaked for 28 days after being submitted to elevated temperatures (20 °C, 200 °C, 400 °C, 600 °C). The comparisons among the chloride ion content of concrete penetrated under different compressive stress are shown in Figure 2a–d.

Figure 2 shows that, as the compressive stress ratio increased from zero to 0.3, the chloride ion concentration in the same layer decreased continuously. For example, at depth 2.5 mm, the chloride ion content was decreased by 3.85%, 13.7% and 16.9% at stress ratios 0.1, 0.2, and 0.3, respectively. In general, the bigger the stress ratio, the more significant the decrease in chloride ion content, implying that a stress ratio of 0.3 and below, inhibit chloride ions' invasion.

However, chloride ion concentration of BFRC under different compressive stress ratios after exposure to high temperatures are quite different. The difference in chloride ion content in concrete that was soaked under compression after 28 days can be clearly found. Illustrations for each figure is shown below:

(1) Figure 2b shows that, after being heated to 200 °C, the chloride ion content in BFRC followed almost the same changing rule as for that at the normal temperature. From the outside to the inside layers, the chloride ion concentration presented a fast diminishing trend. However, the chloride ion content after 200 °C was much higher than that at room temperature, because at higher temperatures, the chloride ions are more likely to enter the concrete matrix and the permeability resistance of concrete decreased.

(2) Figure 2c shows that compared to the normal temperature and 200 °C, the content of chloride ions at 400 °C significantly increased. After 400 °C, calcium hydroxide and gel in concrete began to decompose. High-temperature cracks also provided more channels for chloride ion diffusion, and the permeability resistance of the concrete significantly reduced. From the outside to the inside layers, the chloride ion content first decreased before it went up again with increased stress. The chloride ion content was lowest when the stress ratio is 0.1. At stress ratio 0.2, it recovered to that of the no-stress condition. At stress ratio 0.3, it increased again and was higher than that of the no-stress condition. This indicates that the chloride ion concentration in the concrete surface layer suddenly increased when compressive stress was more significant than a certain level. This value is known as the chloride ion penetration compressive stress ratio threshold of concrete [21]. The current study shows that concrete's chloride ion penetration compressive stress ratio threshold at normal temperature is about 0.5. However, after being exposed to a high temperature of 400 °C, the chloride ion

penetration compressive stress ratio threshold is between 0.1 and 0.2. This result has significant implications for concrete structures after a fire disaster.

(3) BFRC specimens which were heated to 600 °C, under different stress levels (Figure 2d) shows that the chloride ion content of BFRC as a whole was significantly higher compared with that of lower temperatures. After 600 °C, a large amount of calcium hydroxide and gel in the concrete decomposed, density decreased, and high-temperature cracks continued to expand and penetrate, providing more channels for chloride ion diffusion. The chloride ion penetration compressive stress ratio threshold for BFRC disappeared after experiencing a high temperature of 600 °C, and regardless of the load, this had a negative impact on the chloride ion diffusion resistance of concrete.

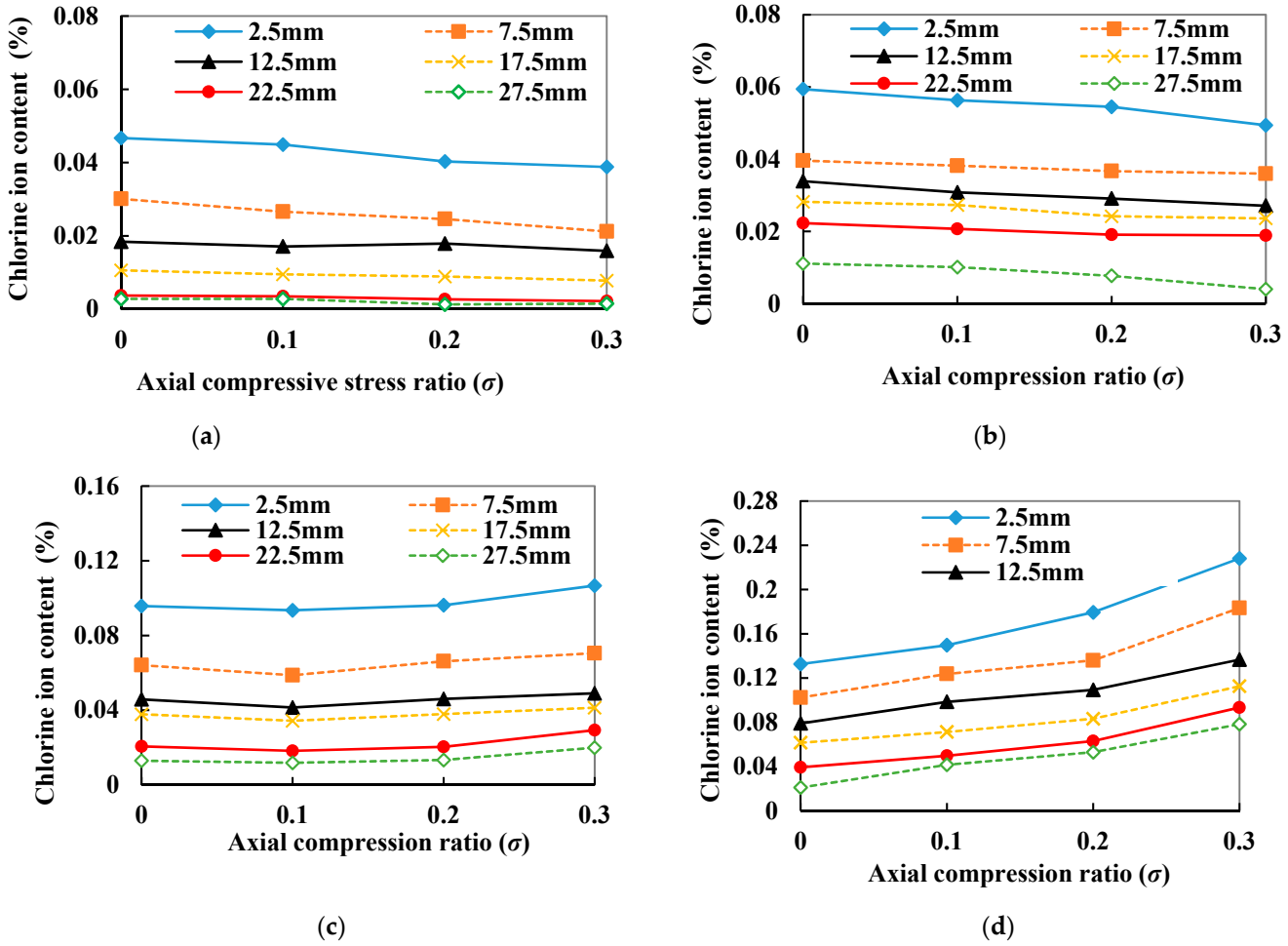

Figure 2. Chloride ion content of concrete with respect to different compressive stress ratios. (**a**) Specimen not heated, (**b**) Specimen soaked after 200 °C, (**c**) Specimen soaked after 400 °C, (**d**) Specimen soaked after 600 °C.

3.2. Effect of Elevated Temperatures on Chloride Ion Diffusion Coefficient

The chloride ion diffusion coefficient can reflect the chloride ion penetration speed in concrete. Additionally, it is generally considered to comply with the analytical solution of Fick's second law. The equation shows the chloride ion content of concrete under various working conditions. By analyzing the chloride ion content of concrete under various working conditions, the chloride ion diffusion coefficient D is obtained, as shown in Table 2.

$$C = C_s\left[1 - \mathrm{erf}\frac{x}{2\sqrt{D}}\right] \quad (1)$$

Table 2. Chloride ion diffusion coefficient of concrete.

Temperature	Axial Compression Ratio ($\times 10^{-11}$)				Erosion Time
	0	0.1	0.2	0.3	
20 °C	3.51	3.27	3.54	3.16	28 days
200 °C	5.28	5.36	5.60	5.54	
400 °C	7.37	6.68	7.20	8.64	
600 °C	9.42	11.1	13.3	15.6	
20 °C	2.03	1.95	1.98	1.96	56 days
200 °C	3.96	3.71	3.37	3.31	
400 °C	5.81	4.61	5.41	6.66	
600 °C	7.88	9.53	11.8	14.4	
20 °C	1.29	1.18	1.33	1.31	84 days
200 °C	2.66	2.30	2.70	2.52	
400 °C	4.59	4.05	4.90	5.71	
600 °C	7.24	8.93	11.3	13.9	

The chloride ion diffusion coefficient of concrete subjected to different elevated temperatures after 28 days of erosion was explored. The changes of the coefficient with different temperatures are shown in Figure 3. The diffusion coefficient of chloride ions increased exponentially with the increase of temperature, and the chloride ions penetrated comparatively faster when the specimen was under stronger compression.

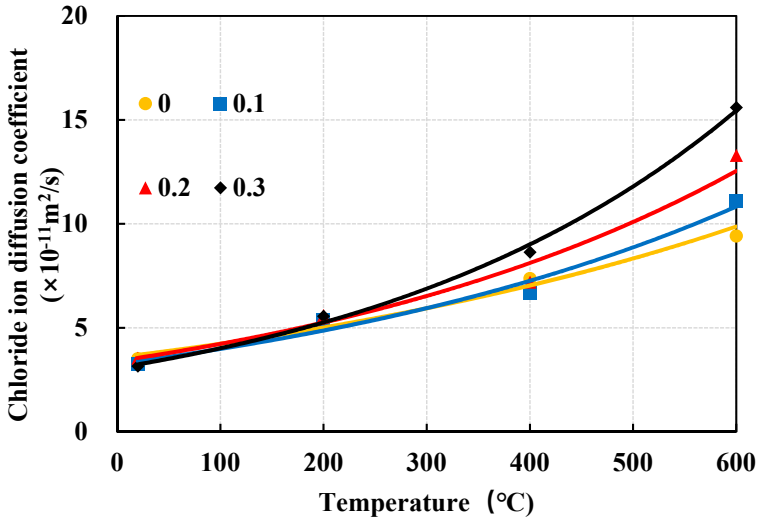

Figure 3. Chloride ion diffusion coefficients with different temperatures after 28 days of erosion.

To describe the influence of high temperatures on the diffusion coefficient of chloride ions, the influence coefficient α is introduced in this paper in Equation (2).

$$\alpha = D_T / D_{20\,^\circ\mathrm{C}} \tag{2}$$

For the conditions without load, the calculation formula of the chloride ion diffusion influence coefficient at high temperatures of concrete is obtained:

$$\alpha = 3.5734 e^{0.0017T} \tag{3}$$

3.3. Effect of Stress Level on Chloride Ion Diffusion Coefficient

Taking the 28-day-eroded concrete as the research object, the chloride ion diffusion coefficient under different compressive stress ratios was determined, as shown in Figure 4.

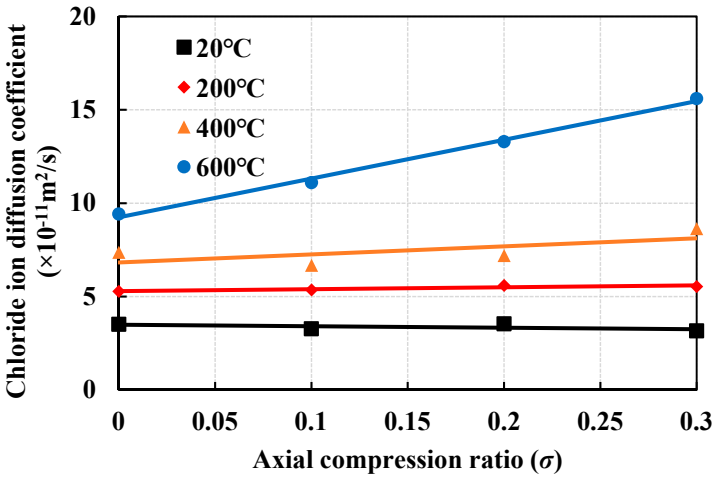

Figure 4. Chloride ion diffusion coefficient with respect to different compressive stress ratios.

Figure 4 shows that the chloride ion diffusion coefficient at 20 °C and 200 °C followed basically the same trend. As the compressive stress ratio increased, the chloride ion diffusion coefficient of concrete under the action of 0.1σ and 0.2σ was slightly lower than that under no stress at 400 °C. However, it was higher under the action of 0.3σ. The chloride ion diffusion coefficient increased linearly at 600 °C.

The compression influence factor β on the chloride ion diffusion coefficient was obtained:

$$\beta = D_\sigma / D_{\sigma=0} \quad (4)$$

The calculated value of the compression influence factor β on the chloride ion diffusion coefficient at different temperatures is shown in Table 3. The compression influence factors of other compressive stress ratios can be obtained by linear interpolation.

Table 3. The compression influence factor β on chloride ion diffusion coefficient.

Axial Compression Ratio	Temperature/°C			
	20	200	400	600
0.1	1	1	1	1.105
0.2	1	1	1	1.412
0.3	1	1	1.173	1.656

3.4. Effect of Erosion Time on Chloride Ion Diffusion Coefficient

Figure 5 shows the evolution of the chloride ion diffusion coefficient of concrete after different temperatures. Concrete's chloride ion diffusion coefficient at different elevated temperatures exhibits a gradual attenuation law with erosion days.

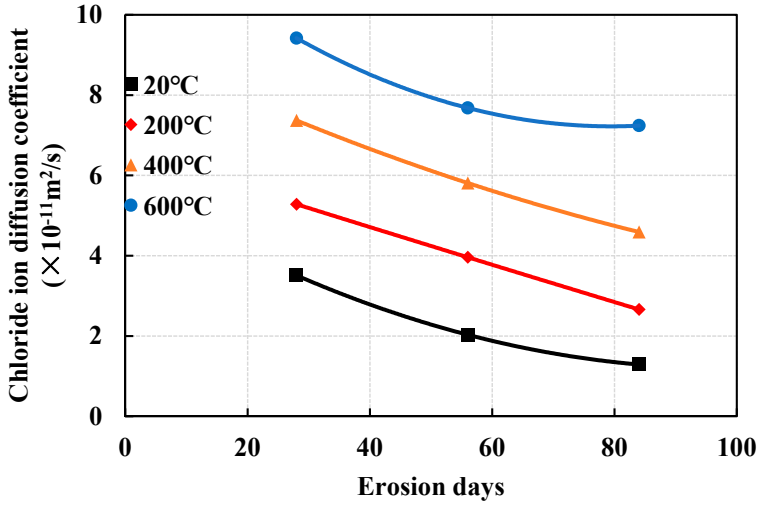

Figure 5. Chloride in diffusion coefficient with erosion days.

Based on the diffusion coefficient of the chloride ion proposed by Mangat and Molloy [21], the recovery factor (m_T) on the chloride ion diffusion coefficient of concrete after heating was introduced:

$$\frac{D_t}{D_{t0}} = \left(\frac{t_0}{t}\right)^{m_T} \tag{5}$$

Using 28 days as the reference for erosion days, the linear relationship between the recovery factor and the temperature was obtained by fitting Figure 5.

$$m_T = -0.0011T + 0.8901 \tag{6}$$

Chloride ion diffusion coefficient of concrete of different erosion days with respect to different compressive stress ratios are shown in Figure 6. It was evident that the influence was minimal when the stress ratio was 0.2 and below, at 20 °C, 200 °C, and 400 °C. The curves differed significantly when the stress ratio was 0.3 at 400 °C and for all the stress ratios at 600 °C if only the chloride ion diffusion recovery coefficient was considered. To make sure the model was accurate, the compressive stress ratio correction factor n_σ was proposed:

$$\frac{D_t}{D_{t0}} = \left(\frac{t_0}{t}\right)^{m_T \cdot n_\sigma} \tag{7}$$

As shown in Figure 7, the value of $\left(\frac{t_0}{t}\right)$ at 400 °C and 600 °C for each stress was obtained by a fitting method according to Equation (7), and divided by the value under no stress. The compressive stress ratio correction factor n_σ is listed in Table 4.

Table 4. Compressive stress ratio correction factor for chloride ion diffusion coefficient.

Axial Compressive Ratio	Temperature/°C			
	20	200	400	600
	n_σ	n_σ	n_σ	n_σ
0.1	1	1	1	0.902
0.2	1	1	1	0.629
0.3	1	1	0.893	0.445

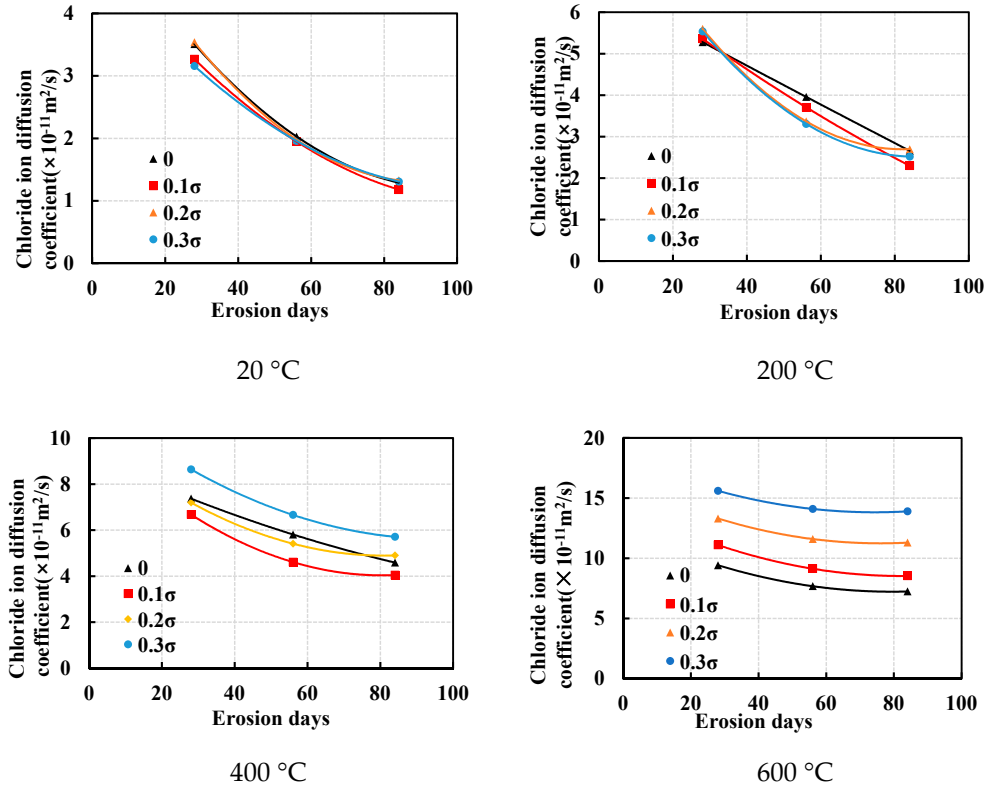

Figure 6. Chloride ion diffusion coefficient of different erosion days with respect to different compressive stress ratios.

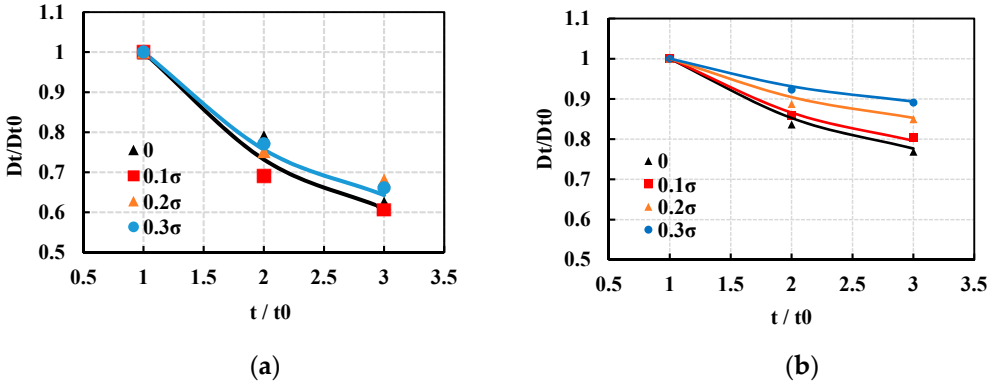

Figure 7. Influence coefficient of the compressive stress ratio. (**a**) n_σ after 400 °C, (**b**) n_σ after 600 °C.

3.5. Chloride Ion Diffusion Coefficient Model and Its Validation

According to Formulas (2), (4), (5), and (7) and the relevant results of the test data, the calculation model of the chloride ion diffusion coefficient of concrete after high temperature-load coupling erosion was proposed. It is shown as follows:

$$D_{t,T,\sigma} = \alpha \cdot \beta \cdot D_{t0} \cdot \left(\frac{t0}{t}\right)^{m_T \cdot n_\sigma} \tag{8}$$

Presently, there are no reports on the chloride ion penetration mechanism in BFRC under the coupling effect of elevated temperatures and loads. In order to verify the accuracy and availability of this model, experimental data from Chen [22] and Ma et al. [23] was utilized. Variation between the chloride ion diffusion coefficients using the proposed model and the chloride ion diffusion coefficients from the test results in the two aforementioned studies for erosion days and temperature changes is shown in Figure 8a,b.

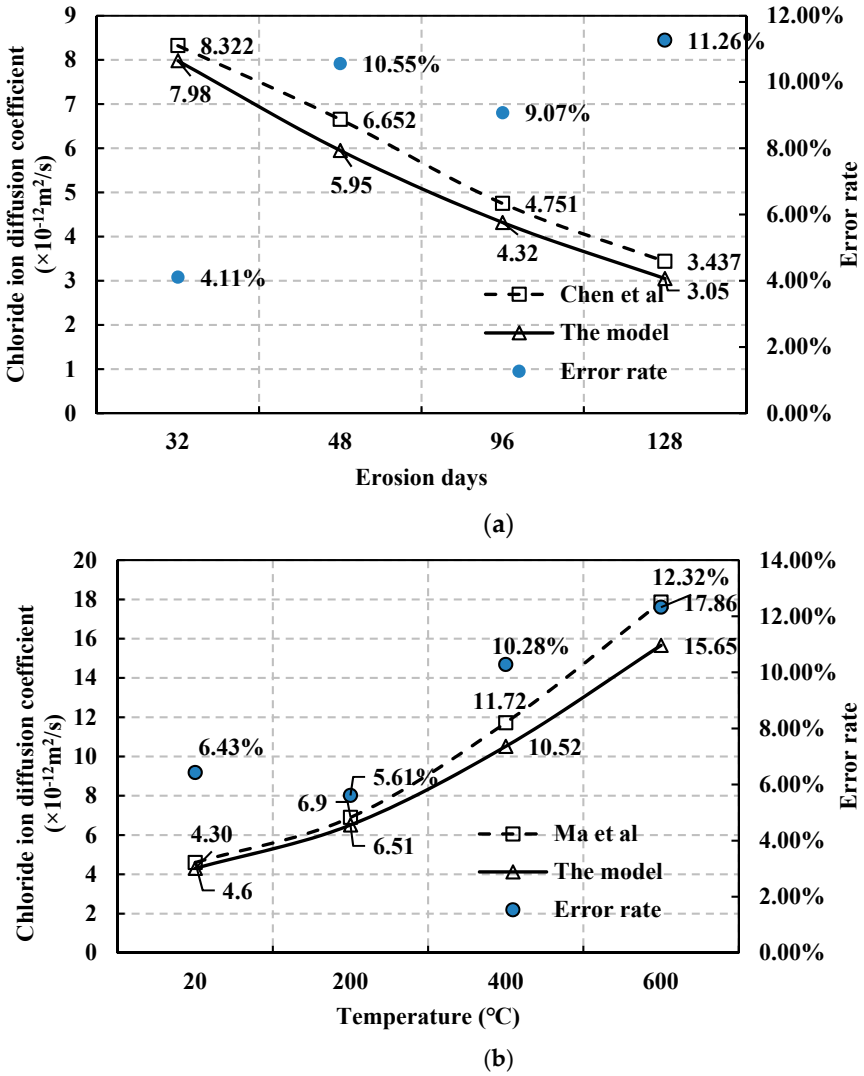

Figure 8. Variation of chloride ion diffusion coefficients using the proposed model in comparison with the test results in the literature: (**a**) compared with the test results of Chen et al. [22]; (**b**) compared with the test results of Ma et al. [23].

In comparison with the references, we focused on the consistency of the changing trend of chloride ion diffusion coefficient, and the differences between them are reasonable. It can be seen that the model differs slightly from the result of Chen [22] and Ma et al. [23] due to fiber addition and experimental methods.

Chen [22] studied the chloride ion penetration of concrete with slag. Due to the excellent stick effect of basalt fiber, the calculated data from the model was slightly lower than the experimental data. Figure 8a shows a better chloride ion penetration resistance of BFRC than slag concrete.

Ma et al. [23] analyzed the chloride ion penetration of recycled aggregate concrete after elevated temperatures. The increasing trend shown in the model and the test results coincided. However, reasonable deviations appeared at elevated temperatures, especially after 300 °C. This is because the model was proposed based on BFRC, which greatly diminishes cracks in concrete when submitted to high temperatures.

4. Conclusions

This paper introduced the research results on the chloride ion penetration mechanism in BFRC and a corresponding calculation model under a thermal-load coupling effect. The following conclusions are drawn:

(1) Chloride ion content at the same depth shows an increasing linear trend with an increase in the heating temperature. Additionally, the chloride ion penetration resistance of concrete decreases significantly between 400 °C and 600 °C.

(2) The chloride ion content in BFRC after being exposed to different elevated temperatures varies significantly with increasing stress:

   (a) The compressive stress of 0.3σ and less can inhibit the entry of chloride ions into concrete and improve the impermeability of concrete at 20 °C and 200 °C. In this instance, the compressive stress ratio threshold of concrete is more significant than 0.3;

   (b) After heating to the temperature of 400 °C, the chloride ion content of BFRC at the same depth from the surface layer to the inner layer first decreases and then increases with the increase in the compressive stress ratio. At this time, the compressive stress ratio threshold of the concrete under chloride ion penetration is between 0.1 and 0.2;

   (c) After heating to a temperature of 600 °C, the chloride ion content of BFRC at the same depth from the surface layer to the inner layer increases with an increase in the compressive stress ratio, and there is no decline stage. The compressive stress ratio threshold of concrete disappears after heating to the elevated temperature of 600 °C.

(3) A calculation model for the chloride ion diffusion coefficient of BFRC under elevated thermal-load coupling effect is proposed, which provides a certain reference for the durability evaluation of elevated temperature damaged BFRC service with damage.

Author Contributions: Conceptualization, L.L. and S.W.; Methodology and writing, Y.Q.; Simulation, G.Y.; review and editing, Q.Z. and J.-H.D. All authors have read and agreed to the published version of the manuscript.

Funding: This research was funded by the NSFC (Grant No. 51808544) and the Research Fund for Doctoral Program of Higher Education of China (Grant No. 2016M601911).

Institutional Review Board Statement: Not applicable.

Informed Consent Statement: Informed consent was obtained from all subjects involved in the study.

Conflicts of Interest: The authors declare no conflict of interest.

Notation

x	The depth from the surface
C	The chloride ion concentration
C_s	The surface concentration of chloride ion
D	Chloride ion diffusion coefficient
α	Elevated temperature influence the coefficient of chloride ion diffusion
D_T	Chloride ion diffusion coefficient of concrete at T °C (m^2/s)
$D_{20\,^\circ C}$	Chloride ion diffusion coefficient of concrete at 20 °C (m^2/s)
T	Temperature (°C)
t	Erosion days
β	Influence coefficient of Chloride ion diffusion in compression
D_σ	Chloride ion diffusion coefficient of concrete when the continuous compressive stress ratio is σ (m^2/s)
$D_{\sigma=0}$	Chloride ion diffusion coefficient of concrete without stress (m^2/s)
D_t	Chloride ion diffusion coefficient of concrete at erosion in t days (m^2/s)
D_{t0}	Chloride ion diffusion coefficient of concrete in $t0$ day (m^2/s)
m_T	Recovery coefficient of chloride ion diffusion coefficient in concrete after T °C
n_σ	Modification coefficient of chloride ion diffusion coefficient in concrete under compressive stress ratio σ
$D_{t,T,\sigma}$	Chloride ion diffusion coefficient in t days under thermal-load coupling erosion

References

1. Anwar, H.; Khandakar, M. Macro-and Microstructural Investigations on Strength and Durability of Pumice Concrete at High Temperature. *J. Mater. Civ. Eng.* **2006**, *18*, 527–536. [CrossRef]
2. Jin, Z.Q.; Zhao, X.; Zhao, T.J.; Li, J.Q. Chloride ions transportation behavior and binding capacity of concrete exposed to different marine corrosion zones. *J. Constr. Build Mater.* **2018**, *177*, 170–183.
3. Li, Y.; Chen, X.H.; Zhang, G.S. A study on effects of water-cement ratio and crack width on chloride ion transmission rate in concrete. *Comput. Concrete* **2017**, *19*, 387–394. [CrossRef]
4. Fu, C.Q.; Ling, Y.F.; Ye, H.L. Chloride resistance and binding capacity of cementitious materials containing high volumes of fly ash and slag. *J. Mag. Concrete Res.* **2021**, *73*, 55–68. [CrossRef]
5. Djerbi, A.; Bonnet, S.; Khelidj, A.; Baroghel-Bouny, V. Influence of traversing crack on chloride diffusion into concrete. *J. Cem. Concrete Res.* **2008**, *38*, 877–883. [CrossRef]
6. Wang, H.L.; Dai, J.G.; Sun, X.Y.; Xiao, Y.; Zhang, X.L. Characteristics of concrete cracks and their influence on chloride penetration. *Constr. Build. Mater.* **2016**, *107*, 216–225. [CrossRef]
7. Mitsuo, O.; Yuki, S.; Kentaro, F.; Tetsura, K.; Parajuli, S.S. Estimation of chloride diffusion coefficients of high-strength concrete with synthetic fibers after fire exposure. *J. Constr. Build. Mater.* **2017**, *143*, 322–329.
8. Okan, K. Transport properties of high volume fly ash or slag concrete exposed to high temperature. *J. Constr. Build. Mater.* **2017**, *152*, 898–906.
9. Bao, J.W.; Wang, L.C. Combined effect of water and sustained compressive loading on chloride penetration into concrete. *J. Constr. Build. Mater.* **2017**, *156*, 708–718. [CrossRef]
10. Sun, J.Y.; Lu, L.G. Coupled effect of axially distributed load and carbonization on permeability of concrete. *J. Constr. Build. Mater.* **2015**, *79*, 9–13. [CrossRef]
11. Lim, C.; Gowripalan, N.; Sirivivatnanon, V. Microcracking and chloride permeability of concrete under uniaxial compression. *J. Cem. Concr. Compos.* **2000**, *22*, 353–360. [CrossRef]
12. Chandramouli, K.; Srinivasa, R.P.; Seshadri, S.T.; Pannirselvam, N.; Sravana, P. Rapid chloride permeability test for durability studies on glass fibre reinforced concrete. *J. Eng. Appl. Sci.* **2010**, *5*, 67–71.
13. Liu, J.; Jia, Y.; Wang, J. Calculation of chloride ion diffusion in glass and polypropylene fiber-reinforced concrete. *J. Constr. Build. Mater.* **2019**, *215*, 875–885. [CrossRef]
14. Scheffler, C.; Förster, T.; Mader, E.; Heinrich, G.; Hempel, S.; Mechtcherine, V. Aging of alkali-resistant glass and basalt fiber in alkaline solutions: Evaluation of the failure stress by Weibull distribution function. *J. Non Cryst. Solids* **2009**, *355*, 2588–2595. [CrossRef]
15. Sim, J.; Park, C.; Moon, D.Y. Characteristics of basalt fiber as a strengthening material for concrete structures. *Compos. Part B Eng.* **2005**, *36*, 504–512. [CrossRef]
16. Mohammadyan-Yasouj, S.E.; Abbastabar Ahangar, H.; Ahevani Oskoei, N.; Shokravi, H.; Rahimian Koloor, S.S.; Petru, M. Thermal Performance of Alginate Concrete Reinforced with Basalt Fiber. *Crystals* **2020**, *10*, 7799. [CrossRef]
17. Zhang, J.Z.; Wang, J.Z.; Kong, D.Y. Chloride diffusivity analysis of existing concrete based on Fick's second law. *J. Wuhan Univ. Technol.* **2010**, *5*, 142–146. [CrossRef]
18. Sun, Y.M.; Liang, M.T.; Chang, T.P. Time/depth dependent diffusion and chemical reaction model of chloride transportation in concrete. *J. Appl. Math Model* **2012**, *36*, 1114–1122. [CrossRef]
19. Ann, K.Y.; Hong, S.I. Modeling chloride transport in concrete a pore and chloride binding. *Aci. Mater. J.* **2018**, *115*, 595–604. [CrossRef]
20. JGJ55-2011. *Specification for Mix Proportion Design of Ordinary Concrete*; China Architecture & Building Press: Beijing, China, 2011. (In Chinese)
21. Mangat, P.S.; Molloy, B.T. Prediction of long term chloride concentration in concrete. *J. Mater. Struct.* **1994**, *27*, 338–346. [CrossRef]
22. Chen, W.G.; Zhu, H.T.; He, Z.H.; Lin, Y.; Zhao, L.P.; Wen, C.C. Experimental investigation on chloride-ion penetration resistance of slag containing fiber-reinforced concrete under drying-wetting cycles. *J. Constr. Build. Mater.* **2021**, *274*, 829–841. [CrossRef]
23. Ma, Z.M.; Liu, M.; Tang, Q.; Liang, C.F.; Duan, Z.H. Chloride permeability of recycled aggregate concrete under the coupling effect of freezing-thawing, elevated temperature or mechanical damage. *J. Constr. Build. Mater.* **2020**, *237*, 648–659. [CrossRef]